nature biomedical engineering

Supplementary information

https://doi.org/10.1038/s41551-025-01509-2

Solid tumour CAR-T cells engineered with fusion proteins targeting PD-L1 for localized IL-12 delivery

In the format provided by the authors and unedited

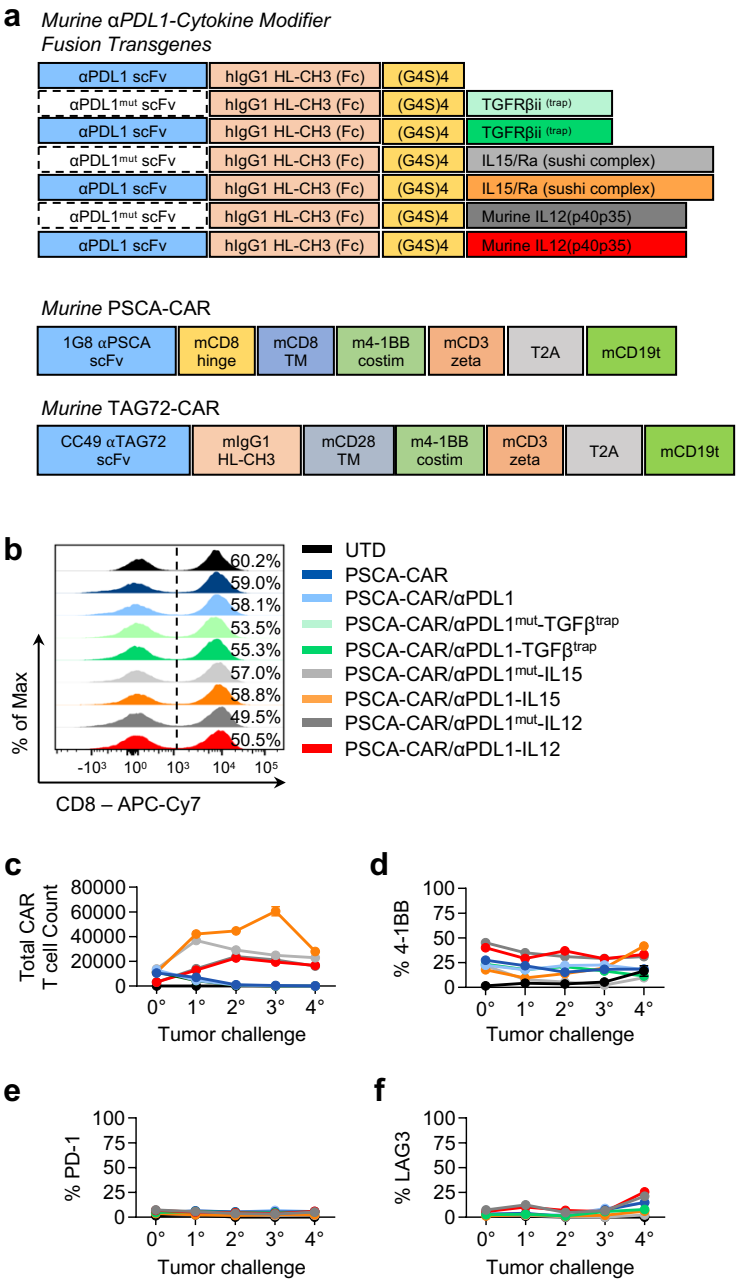

Figure S1: Murine construct designs and additional data related to Figure 1. (a) Construct designs used for murine αPDL1-cytokine modifier (TGFβRii $^{(trap)}$, IL15/Ra (sushi complex), or murine IL12(p40p35)) fusion transgenes and relevant controls, fully murine PSCA-targeting and murine TAG72-targeting CAR T cell constructs. All anti-PDL1 scFv's are derived from Avelumab which is cross reactive to mouse PD-L1. **(b)** Flow cytometry histograms of CD8+ percentage on indicated untransduced (UTD) or PSCA-CAR conditions. Flow cytometry analysis of percentage

(c) total CAR+ T cell count per tumor re-challenge, **(d)** 4-1BB+, **(e)** PD-1+, and **(f)** LAG3+ expression, n = 3 technical replicates per condition and representative of two independent experiments. Data are presented as mean ±SEM. Unless otherwise indicated, p-values for pairwise comparisons were generated using an unpaired two-tailed Student's t-test with assumption of unequal variance where * $p<0.05$, ** $p<0.01$, *** $p<0.001$, **** $p<0.0001$. All data in figure are representative of at least two independent experiments.

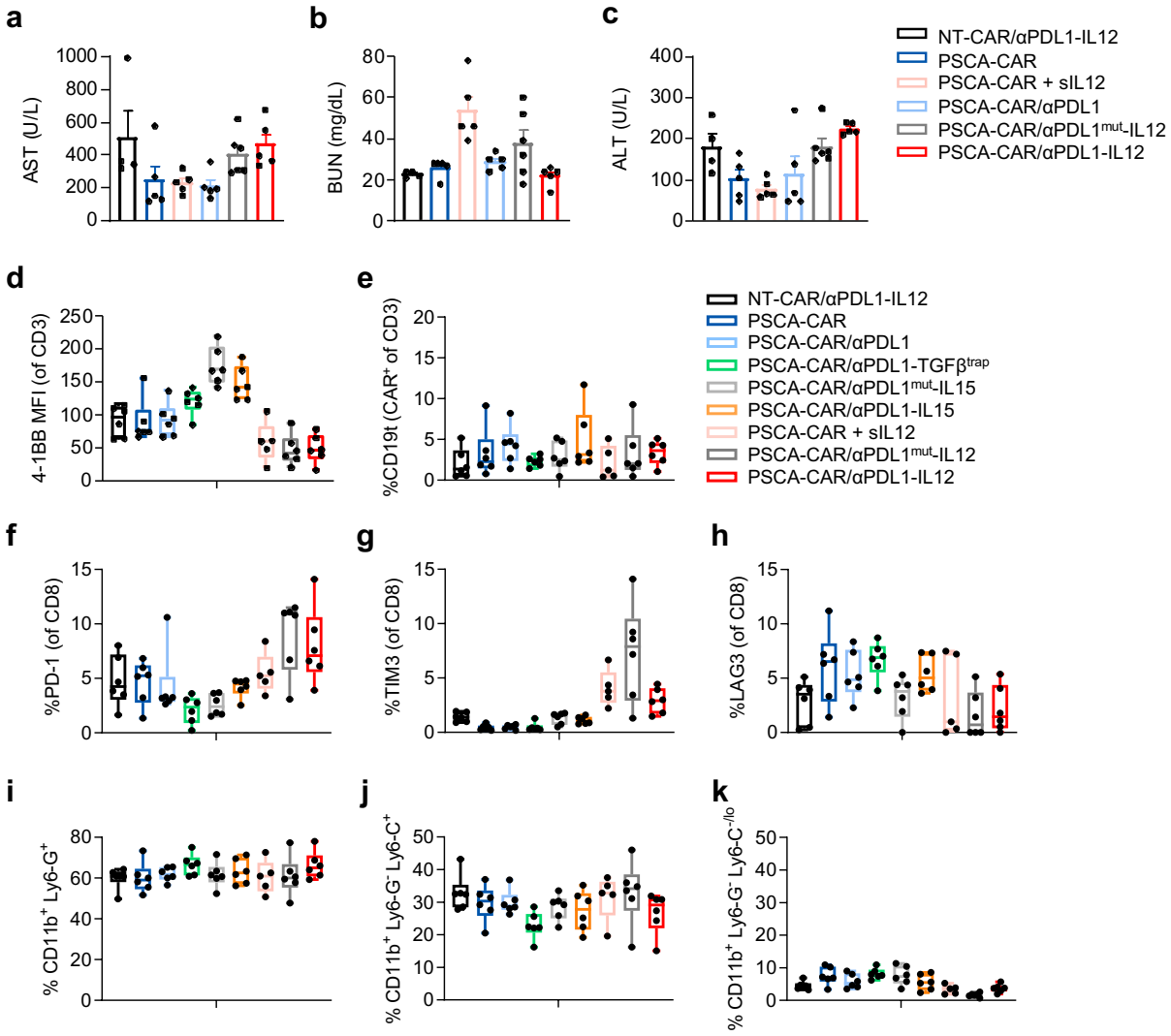

Figure S2: Additional data related to Figure 2. (a-c) Quantification of AST (U/L) **(a)**, BUN (mg/dL) **(b)**, and ALT (U/L) **(c)** in serum from indicated treatment groups, n = 4 mice (NT-CAR), n = 6 mice (PSCA-CAR/αPLD1^{mut}-IL12), n = 5 mice per group for all others. Flow cytometry analysis of peripheral blood 6 days post T cell injection, n = 6 mice per group, except PSCA-CAR + sIL12 (n = 5 mice) for **(d)** 41BB MFI (of CD3+ T cells), **(e)** CD19t+ (% of CAR+ T cells) **(f)** PD-1 (% of CD8+ T cells), **(g)** TIM3 (% of CD8+ T cells) **(h)** LAG3 (% of CD8+ T cells), **(i)** percentage of CD11b+Ly6G+ granulocytes, **(j)** percentage of CD11b^{+}Ly6-G^{-}Ly6-C^{+} monocytes, and **(k)** percentage of CD11b^{+}Ly6-G^{-}Ly6-C$^{-/lo}$ monocytes. Box plots presented with center line mean value and whiskers from min to max. Data are presented as mean ±SEM. All data in figure are representative of at least two independent experiments.

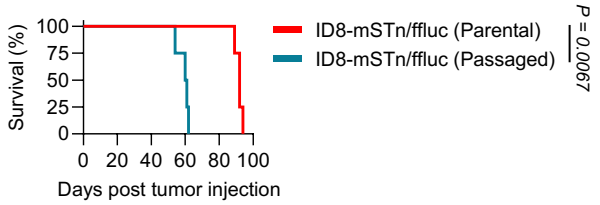

Figure S3: Survival curves for parental and passaged ID8-mSTn/ffluc-bearing mice. Kaplan-Meier survival plot for mice engrafted i.p. with either $5.0x10^6$ parental ID8-mSTn/ffluc or aggressive passage ID8-mSTn/ffluc. n = 4 mice per group, p-value using a Log-rank (Mantel-Cox) test. Data presented representative from of two independent experiments.

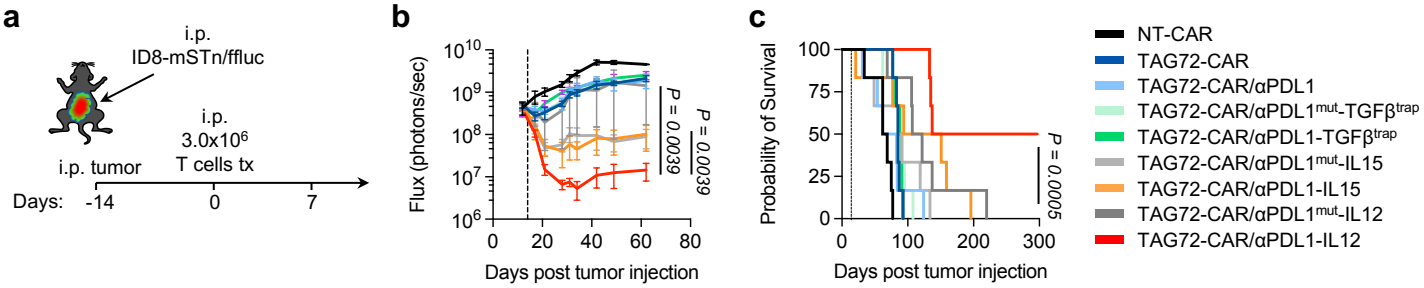

Figure S4: Therapeutic efficacy of TAG72-CAR T cells with bifunctional fusions. (a) Schematic of intraperitoneal (i.p.) ID8-mSTn/ffluc tumor model treatment and harvest timepoints. **(b)** Tumor flux quantification of tumor-bearing mice treated with non-targeting CAR (NT), TAG72-CAR alone, or TAG72-CAR engineered with αPDL1, αPDL1^{mut}-TGFβ^{trap} αPDL1-TGFβ^{trap}, αPDL1^{mut}-IL15, αPDL1-IL15, αPDL1^{mut}-IL12, or αPDL1-IL12 (3.0x10^6 CAR+ cells; i.p.). P-value compares PSCA-CAR/αPDL1^{mut}-IL12 and PSCA-CAR/αPDL1-IL12 treatment and PSCA-CAR/αPDL1-IL15 and PSCA-CAR/αPDL1-IL12, n = 6 mice per group. **(c)** Kaplan-Meier survival plot. Statistical comparisons are of TAG72-CAR/αPDL1^{mut}-IL12 vs. TAG72-CAR/αPDL1-IL12 using a Log-rank (Mantel-Cox) test, n = 6 mice per group (b-c). Data are presented as mean ±SEM. Unless otherwise indicated, pairwise comparisons were generated using an un-paired two-tailed Student's t test with assumption of unequal variance where * p<0.05, ** p<0.01, *** p<0.001, **** p<0.0001. Data presented representative from of two independent experiments.

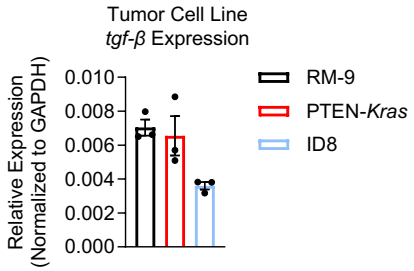

Figure S5: RT-PCR analysis of murine *tgf-β* gene expression in murine tumor cell lines. Data are presented as mean ±SEM. n = 3 technical replicates per condition**.** Data presented representative from of two independent experiments.

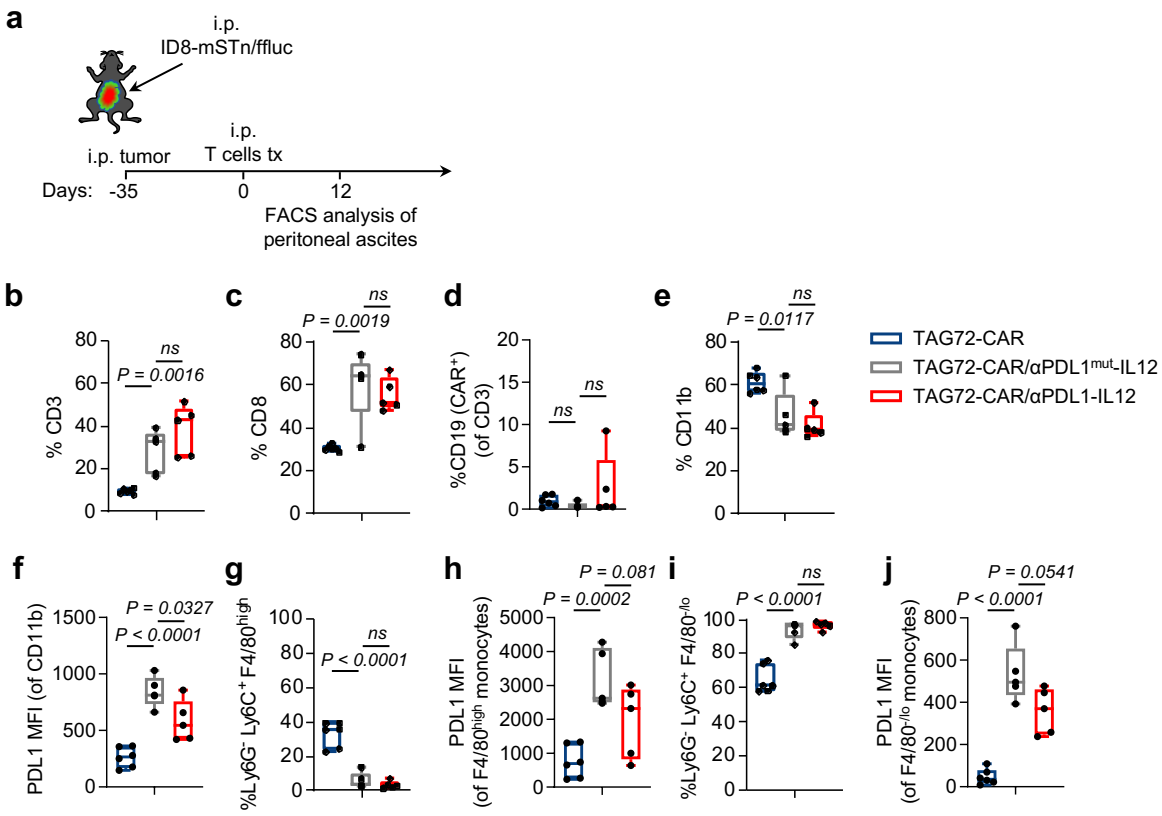

Figure S6: Additional data related to Figure 3. (a) Illustration of intraperitoneal (i.p.) ID8-mSTn/ffluc tumor model engraftment, day 35 treatment, and harvest timepoint at day 12 post T cell injection as indicated. **(b-e)** Flow cytometry analysis of peritoneal ascites collected at day 12 post T cell injection, percentage of CD3+ **(b)**, CD8+ **(c)**, CD19t+ (CAR+) of total T cells **(d)**, and CD11b+ **(e)**. **(f)** Mean fluorescence intensity (MFI) of PDL1 on total CD11b+ myeloid cells, **(g)** percentage of $CD11b^{+}Ly6\text{-}G^{-}Ly6\text{-}C^{+}F4/80^{high}$ monocytes, **(h)** MFI of PDL1 on $F4/80^{high}$ monocytes, **(i)** percentage of $CD11b^{+}Ly6\text{-}G^{-}Ly6\text{-}C^{+}F4/80^{-lo}$ monocytes, and **(j)** MFI of PDL1 on $F4/80^{-/lo}$ monocytes. n = 5 mice per group (TAG72-CAR/αPDL1^{mut}-IL12 and TAG72-CAR/αPDL1-IL12), n = 6 mice per group (TAG72-CAR). Data are presented as mean ±SEM. Unless otherwise indicated, p-values for pairwise comparisons were generated using an un-paired two-tailed Student's t test with assumption of unequal variance where * p<0.05, ** p<0.01, *** p<0.001, **** p<0.0001.

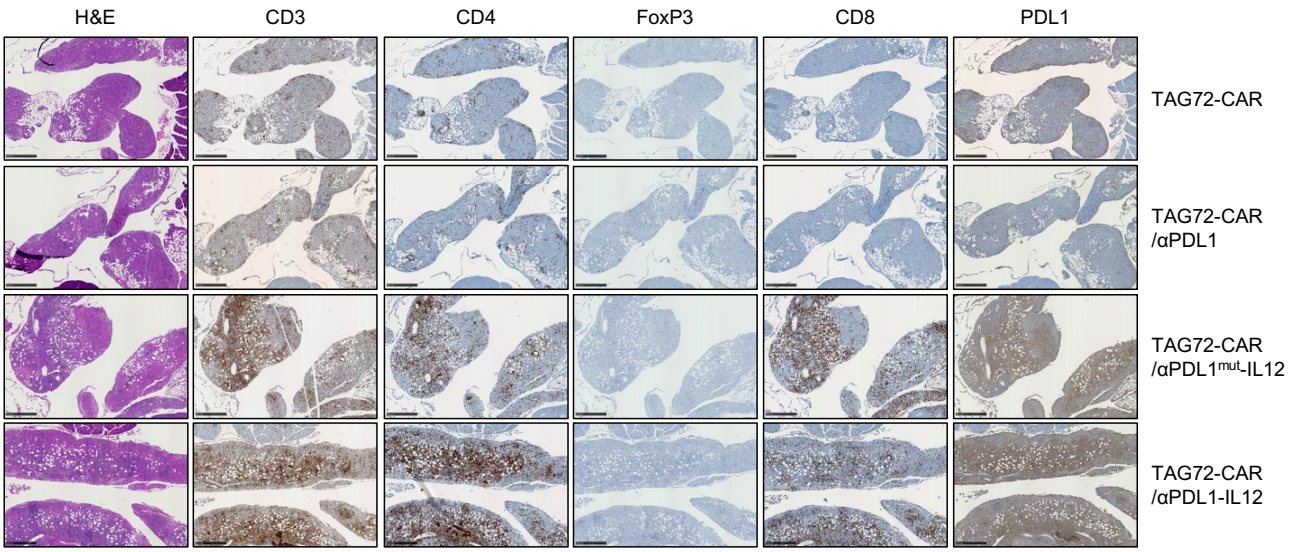

Figure S7: Histology data related to Figure 4. Representative H&E staining and immunohistochemistry of CD3, CD4, FoxP3, CD8, and PDL1 proteins on tumor tissues from ID8-mSTn/ffluc engrafted mice, collected day 7 after T cell injection in indicated treatment groups. Scale bars = 300 μm.

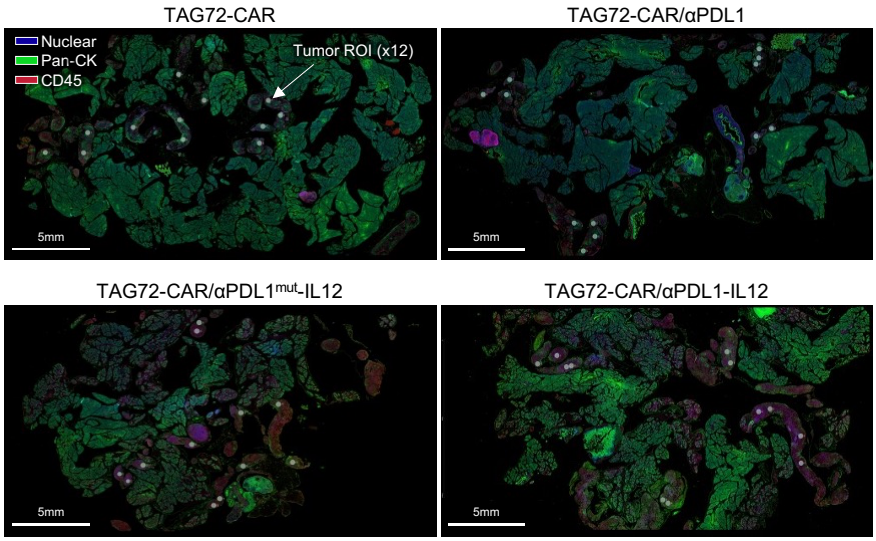

Figure S8: Additional data related to Figure 4. Total tissue Nanostring GeoMx® captured immunofluorescence images and ROI's (white dots; n = 12 representing a minimum of 2 ROI per tumor per mouse, n = 3 mice per group) harvested at day 7 post T cell injection from TAG72-CAR, TAG72-CAR/αPDL1, TAG72-CAR/αPDL1^{mut}-IL12, and TAG72-CAR/αPDL1-IL12 treatment groups. Nuclear stain (blue), Pan-CK (green), CD45 (red). Scale bars = 5 mm.

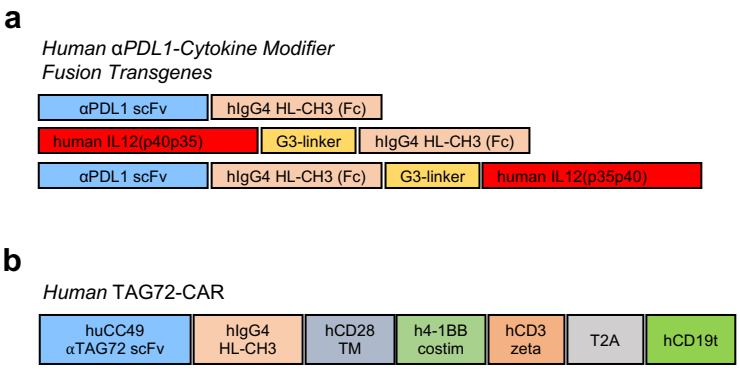

Figure S9: Human construct designs related to Figure 6. (a) Construct designs used for human αPDL1-Fc-humanIL12(p35p40) fusion transgenes and relevant controls hIL12(p35p40)-Fc and αPDL1-Fc. **(b)** Illustration of TAG72-targeting human CAR T cell construct. All anti-PDL1 scFv's are derived from Avelumab.

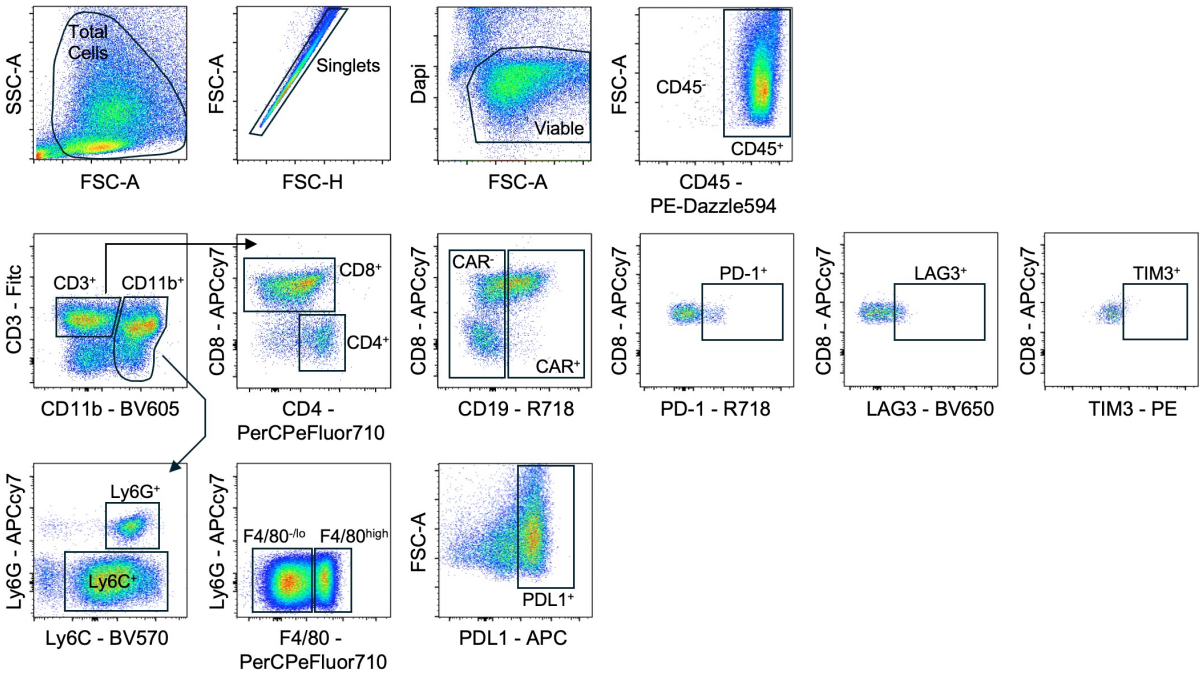

Figure S10: Representative flow cytometry gating strategy used for tumor, ascites, and peripheral blood analyses of immune lymphoid and myeloid populations.

Construct	Amino Acid Sequence
αPDL1 scFv	QSALTQPASVSGSPGQSITISCTGTSSDVGGYNYVSWYQQHPGKAPKLMIYDVSNRPSGVSNRFSGSKSGNTASLTISG LQAEDEADYYCSSYTSSSTRVFGTGTKVTVLGGGGSGGGGSGGGGSEVQLLESGGGLVQPGGSLRLSCAASGFTFSSYI MMWVRQAPGKGLEWVSSIYPSGGITFYADTVKGRFTISRDNSKNTLYLQMNSLRAEDTAVYYCARIKLGTVTTVDYWGQ GTLVTVSS
αPDL1^{Mut} scFv	QSALTQPASVSGSPGQSITISCTGTSSDVGGYNYVSWYQQHPGKAPKLMIYDVSNRPSGVSNRFSGSKSGNTASLTISG LQAEDEADYYCSSYTSSSTRVFGTGTKVTVLGGGGSGGGGSGGGGSEVQLLESGGGLVQPGGSLRLSCAASGFTFSWYG MDWVRQAPGKGLEWVSSIYPSGGITFYADTVKGRFTISRDNSKNTLYLQMNSLRAEDTAVYYCARIKLGTVTTVDYWGQ GTLVTVSS
Human IgG1 (HL-CH3) (Fc)	EPKSCDKTHTCPGGGSSGGGSGGQPREPQVYTLPPSREEMTKNQVSLTCLVKGFYPSDIAVEWESNGQPENNYKTTPPV LDSDGSFFLYSKLTVDKSRWQQGNVFSCSVMHEALHNHYTQKSLSLSPGA
Human IgG4 (HL-CH3) (Fc)	ESKYGPPCPPCPGGGSSGGGSGGQPREPQVYTLPPSQEEMTKNQVSLTCLVKGFYPSDIAVEWESNGQPENNYKTTPPV LDSDGSFFLYSRLTVDKSRWQEGNVFSCSVMHEALHNHYTQKSLSLSLGK
(G4S)4 Linker	GGGGSGGGGSGGGGSGGGGS
G3 Linker	GGG
Murine IL-12 (p40p35)	MWELEKDVYVVEVDWTPDAPGETVNLTCDTPEEDDITWTSDQRHGVIGSGKTLTITVKEFLDAGQYTCHKGGETLSHSH LLLHKKENGIWSTEILKNFKNKTFLKCEAPNYSGRFTCSWLVQRNMDLKFNIKSSSSSPDSRAVTCGMASLSAEKVTLD QRDYEKYSVSCQEDVTCPTAEETLPIELALEARQQNKYENYSTSFFIRDIIKPDPPKNLQMKPLKNSQVEVSWEYPDSW STPHSYFSLKFFVRIQRKKEKMKETEEGCNQKGAFLVEKTSTEVQCKGGNVCVQAQDRYYNSSCSKWACVPCRVRSGGG GSGGGGSGGGGSRVIPVSGPARCLSQSRNLLKTTDDMVKTAREKLKHYSCTAEDIDHEDITRDQTSTLKTCLPLELHKN ESCLATRETSSTTRGSCLPPQKTSLMMTLCLGSIYEDLKMYQTEFQAINAALQNHNHQQIILDKGMLVAIDELMQSLNH NGETLRQKPPVGEADPYRVKMKLCILLHAFSTRVVTINRVMGYLSSA
Human IL-12 (p35p40)	ARNLPVATPDPGMFPCLHHSQNLLRAVSNMLQKARQTLEFYPCTSEEIDHEDITKDKTSTVEACLPLELTKNESCLNSR ETSFITNGSCLASRKTSFMMALCLSSIYEDSKMYQVEFKTMNAKLLMDPKRQIFLDQNMLAVIDELMQALNFNSETVPQ KSSLEEPDFYKTKIKLCILLHAFRIRAVTIDRVMSYLNASVPGVGVPGVGIWELKKDVYVVELDWYPDAPGEMVVLTCD TPEEDGITWTLDQSSEVLGSGKTLTIQVKEFGDAGQYTCHKGGEVLSHSLLLLHKKEDGIWSTDILKDQKEPKNKTFLR CEAKNYSGRFTCWWLTTISTDLTFSVKSSRGSSDPQGVTCGAATLSAERVRGDNKEYEYSVECQEDSACPAAEESLPIE VMVDAVHKLKYENYTSSFFIRDIIKPDPPKNLQLKPLKNSRQVEVSWEYPDTWSTPHSYFSLTFCVQVQGKSKREKKDR VFTDKTSATVICRKNASISVRAQDRYYSSSWSEWASVPCS
IL15/Ra (sushi complex)	ITCPPPMSVEHADIWVKSYSLYSRERYICNSGFKRKAGTSSLTECVLNKATNVAHWTTPSLKCIRDPALVHQRSGGGSG GGGSGGGGSGGGGSGGGSLQNWVNVISDLKKIEDLIQSMHIDATLYTESDVHPSCKVTAMKCFLLELQVISLESGDASI HDTVENLIILANNSLSSNGNVTESGCKECEELEEKNIKEFLQSFVHIVQMFINTS
TGFRβii$^{(trap)}$	GIPPHVQKSVNNDMIVTDNNGAVKFPQLCKFCDVRFSTCDNQKSCMSNCSITSICEKPQEVCVAVWRKNDENITLETVC HDPKLPYHDFILEDAASPKCIMKEKKKPGETFFMCSCSSDECNDNIIFSEEYNTSNPD
Murine PSCA-CAR	MLLLVTSLLLCELPHPAFLLIPQVVLTQSPAIMSASPGEKVTMACSASSSVRFIHWYQQKSGTSPKRWIYDTSKLAS GVPTRFSGSGSGTSYSLTISTMEAEDAATYYCQQWSSSPFTFGSGTKLIIKGSTSGGGSGGGSGGGGSSEVQLQQSG AELVRSGASVKLSCTASGFNIKDYYIHWVNQRPDQGLEWIGWIDPENGDTEFVPKFQGKATMTADIFSNTAYLHLSS LTSEDTAVYYCKTGGFWGQGTLVTVSATTTKPVLRTPSPVHPTGTSQPQRPEDCRPRGSVKGTGLDFACDIYIWAPL AGICVALLLSLIITLICSVLKWIRKKFPHIFKQPFKKTTGAAQEEDACSCRCPQEEEGGGGGYELGGGRAKFSRSAE TAANLQDPNQLYNELNLGRREEYDVLEKKRARDPEMGGKQQRRRNPQEGVYNALQKDKMAEAYSEIGTKGERRRGKG HDGLYQGLSTATKDTYDALHMQTLAPRLEGGGEGRGSLLTCGDVEENPGPTRMPSPLPVSFLLFLTLVGGRPQKSLL VEVEEGGNVVLPCLPDSSPVSSEKLAWYRGNQSTPFLELSPGSPGLGLHVGSLGILLVIVNVSDHMGGFYLCQKRPP FKDIWQPAWTVNVEDSGEMFRWNASDVRDLDCDLRNRSSGSHRSTSGSQLYVWAKDHPKVWGTKPVCAPRGSSLNQS LINQDLTVAPGSTLWLSCGVPPVPVAKGSISWTHVHPRRPNVSLLSLSLGGEHPVREMWVWGSLLLLPQATALDEGT YYCLRGNLTIERHVKVIARSAVWLWLLRTGGWIVPVVTLVYVIFCMVSLVAFLYCQRAFILRRKR
Murine TAG72-CAR	QVQLQQSDAELVKPGASVKISCKASGYTFTDHAIHWVKQNPEQGLEWIGYFSPGNDDFKYNERFKGKATLTADKSSS TAYLQLNSLTSEDSAVYFCTRSLNMAYWGQGTSVTVSSGSTSGGGSGGGSGGGGSSDIVMTQSPSSLPVSVGEKVTL SCKSSQSLLYSGNQKNYLAWYQQKPGQSPKLLIYWASTRESGVPDRFTGSGSGTDFTLSISSVETEDLAVYYCQQYY SYPLTFGAGTKLVLKESKYGPPCPPCPGGGSSGGGSGGRPKAPQVYTIPPPKEQMAKDKVSLTCMITDFFPEDITVE WQWNGQPAENYKNTQPIMNTNGSYFVYSKLNVQKSNWEAGNTFTCSVLHEGLHNHHTEKSLSHSPGKFWALVVVAGV LFCYGLLVTVALCVIWTSVLKWIRKKFPHIFKQPFKKTTGAAQEEDACSCRCPQEEEGGGGGYELGGGRAKFSRSAE TAANLQDPNQLYNELNLGRREEYDVLEKKRARDPEMGGKQQRRRNPQEGVYNALQKDKMAEAYSEIGTKGERRRGKG HDGLYQGLSTATKDTYDALHMQTLAPRLEGGGEGRGSLLTCGDVEENPGPTRMPSPLPVSFLLFLTLVGGRPQKSLL VEVEEGGNVVLPCLPDSSPVSSEKLAWYRGNQSTPFLELSPGSPGLGLHVGSLGILLVIVNVSDHMGGFYLCQKRPP FKDIWQPAWTVNVEDSGEMFRWNASDVRDLDCDLRNRSSGSHRSTSGSQLYVWAKDHPKVWGTKPVCAPRGSSLNQS LINQDLTVAPGSTLWLSCGVPPVPVAKGSISWTHVHPRRPNVSLLSLSLGGEHPVREMWVWGSLLLLPQATALDEGT YYCLRGNLTIERHVKVIARSAVWLWLLRTGGWIVPVVTLVYVIFCMVSLVAFLYCQRAFILRRKR

Table S1: Amino acid sequences used to generate bifunctional fusion proteins illustrated in Figure S1a and S9a (murine and human, respectively). Amino acid sequence for murine PSCA-CAR and TAG72-CAR are color coded corresponding to illustrations in Figure S1a.